On the nature of Collinder 121: insights from the low-mass pre-main sequence

Ben Burningham,[1]★ Tim Naylor,[1] R. D. Jeffries[2] and C. R. Devey[2]

[1]*School of Physics, University of Exeter, Stocker Road, Exeter EX4 4QL*
[2]*Department of Physics, Keele University, Keele, Staffordshire ST5 5BG*

ABSTRACT

We present a *VI* photometric catalogue towards the open cluster Cr 121. *XMM–Newton* and *ROSAT* data are used to discover a low-mass pre-main sequence (PMS) along this sightline. de Zeeuw et al. have identified Cr 121 as a moving group, using *Hipparcos* data, at a distance of 592 pc; we reject the scenario that these low-mass PMS stars are associated with that association. By considering the higher mass main sequence stellar membership of the groups along this sightline, the density of low-mass PMS stars and their age spread we argue that the low-mass PMS stars are associated with a young, compact cluster at a distance of 1050 pc. This is consistent with Collinder's original description of Cr 121, and we argue that this distant compact cluster should retain its original designation. The moving group detected by de Zeeuw et al. resembles a foreground association and we agree with Eggen that this should be called CMa OB2.

This study demonstrates that although the de Zeeuw et al. census of OB associations is an invaluable resource for studying local star formation, it must be interpreted in the context of other data when considering structure over distances of the same order as the limits of the *Hipparcos* parallaxes.

Key words: techniques: photometric – stars: formation – stars: low-mass, brown dwarfs – open clusters and associations: Cr 121 – open clusters and associations: CMa OB 2 – X-rays: stars.

1 INTRODUCTION

Collinder 121 (Cr 121) is listed in the New List of OB Associations (Melnik & Efremov 1997) as an OB association at a distance of 540 pc. However, since its first identification as an open cluster of about 1° diameter by Collinder (1931), Cr 121 has had its membership re-assessed a number of times. In this paper we use the low-mass pre-main sequence (PMS) to resolve the long-standing controversy over the nature of Cr 121, and demonstrate the power of the using the low-mass PMS to pick apart structure in OB associations. We also illustrate the difficulties associated with using proper motion and parallax data of limited range in isolation.

The cluster was first discovered as a group of 18–20 main-sequence B stars found within a 40×60 arcmin^2 box. Collinder (1931) used the cluster diameter, along with the mean separation of stars within it, to derive a distance of 1260 pc. Feinstein (1967) studied the cluster using UBV photometry and extended the membership to 40 stars brighter than $V = 7$ within a $10° \times 10°$ box. This group was characterized as an OB association and the position of

the zero-age main sequence (ZAMS) indicated a distance of 630 pc. Already, two very different structures had been described by different authors. Eggen (1981) suggested that the original compact group and the larger OB association may be distinct. Using intermediate-band and Hβ photometry Eggen (1981) placed the compact group, which he referred to as Cr 121, at a distance of 1.17 kpc at an age of 1.5 Myr. The more diffuse group, which Eggen referred to as CMa OB2, was found to be at a distance of 740 pc.

More recently, emphasis has been placed on the use of common motion criteria for defining cluster and association memberships. de Zeeuw et al. (1999) used *Hipparcos* proper motion and parallax data to select a moving group in the direction of Cr 121. They selected 103 stars in a region $13° \times 16°$ in extent, and find a mean distance of 592 ± 28 pc. The presence of an O star, a Wolf–Rayet (WR) star and early-type B stars in the membership list led to an estimated age of ∼5 Myr. Since stars were selected from a large region of sky compared with the original boundaries of the distant interpretation of Cr 121, and the fact the *Hipparcos* parallaxes become unreliable at about 1 kpc, this selection method is biased towards detecting a larger, more diffuse foreground association rather than the distant compact cluster of Collinder (1931). If both groups were present, as suggested by Eggen (1981), only the foreground association would be detected as this

★E-mail: bgb@astro.ex.ac.uk

would represent a large number of stars with common motion at a similar distance, within the reliable domain of *Hipparcos* parallaxes. Dias, Lépine & Alessi (2001) used data from the Tycho2 catalogue to redetermine the mean proper motion of Cr 121, amongst other clusters. This study was restricted to open clusters within 1 kpc, so again was biased towards only detecting the foreground group, and would have been insensitive to any more distant cluster along the same line of sight. Apparently working within the assumption of the de Zeeuw et al. (1999) view of Cr 121 and the Dias et al. (2001) membership list, Dias et al. (2002) determine the distance to Cr 121 as 470 pc with an age of 11 Myr.

Kaltcheva (2000) carried out Strömgren and Hβ photometry of bright B stars within a $5°$ radius of the classical centre $(l, b) = (235°4, -10°4)$ of Cr 121. This revealed a group of stars at 660–730 pc, with characteristics similar to an OB association, and a more compact group of stars at a distance of 1085 pc, which she calls Cr 121. This would indicate that the original cluster Cr 121 is situated at a distance of over 1 kpc, whilst the Cr 121 selected by de Zeeuw et al. (1999) is a less distant OB association.

Inspection of the *ROSAT* Position Sensitive Proportional Counter (PSPC) catalogue revealed a number of X-ray point sources in the vicinity of WR 6, near the centre of the region studied by Kaltcheva (2000) and the original centre of Collinder's cluster. WR 6 is listed as a member of Cr 121 by de Zeeuw et al. (1999), but not by Kaltcheva (2000). The *Hipparcos* parallax for WR 6 of $\pi = 1.74 \pm 0.76$ mas, puts it at a distance of 575 pc.

Low-mass PMS stars are expected to be X-ray bright owing to high levels of coronal activity, as such, X-ray data has been used as a diagnostic tool for identifying low-mass PMS stars (e.g. Naylor & Fabian 1999; Pozzo et al. 2000). The presence of low-mass PMS stars would allow us to fit isochrones to the PMS in a colour–magnitude diagram (CMD), constraining the distance and age of the PMS. With this in mind we have obtained deep *VI* imaging photometry of a region 20 arcmin in radius, covering the central region of the *ROSAT* PSPC field of view (FoV) for the pointings carried out towards WR 6. Since the optical data were obtained, *XMM–Newton* data for this region of sky have become available, allowing us to perform a more sensitive X-ray selection of PMS stars.

The layout of our optical survey is shown in Fig. 1, along with the location of the B stars identified as being members of the more distant group by Kaltcheva (2000) and WR 6. Although our survey region coincides with only two of the B stars identified by Kaltcheva (2000) as members of the more distant cluster, and lies towards the edge of the region enclosed by them, we would still expect to find a significant number of low-mass PMS stars from that group within our survey. Studies of other young clusters and OB associations have always revealed O and B stars located within a sea of low-mass PMS stars, not low-mass PMS stars only within a region enclosed by higher mass stars (e.g. Dolan & Mathieu 2001; Pozzo et al. 2003).

2 OPTICAL DATA

2.1 Observations

The *VI* CCD imaging of 8 13.5-arcmin FoVs centred on WR 6 was carried out using the 0.9-m telescope at the Cerro Tololo Interamerican Observatory (CTIO) in Chile on the night of 2002 February 12/13.

The FoVs were selected to cover the central region of the *ROSAT* PSPC pointings. Each field was observed with short (10, 6 s) and long exposures (300, 180 s) in the *V* and *I* bands in photometric
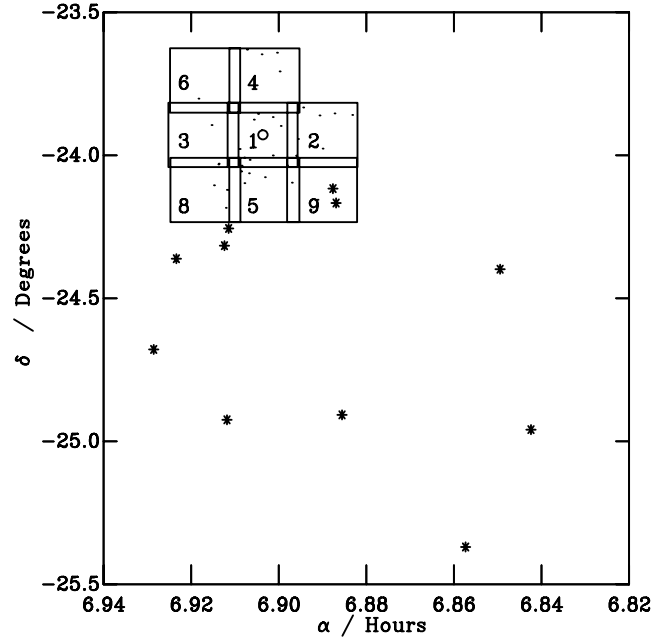
Figure 1. The layout of the fields observed towards WR 6. The square boxes outline the 3.5×13.5 arcmin^2 CTIO 0.9-m fields of view. The 11 B stars listed as members of the more distant association described by Kaltcheva (2000) are marked as asterisks. WR 6 is marked with a circle. The PMS objects discovered here are marked with dots.

conditions. The short exposures were aimed at capturing the brighter stars in each field, which would be saturated in the long exposures. To reduce the number of cosmic ray hits in any one image the long exposures were split into three parts, of 100 s in *V* and 60 s in *I*. The fields were overlapped with each other to provide a check for the internal consistency of the photometry (see Section 2.2). A number of Landolt (1992) standard star fields, containing standards with $-0.6 \leqslant V - I \leqslant 5.8$, were also observed at several times during the night. This ensured adequate calibration over the colour range of interest.

2.2 Data reduction and optimal photometry

The data were reduced, and photometry was performed using the optimal extraction algorithm originally described by Naylor (1998) with its application for constructing CMDs described in depth by Naylor et al. (2002). The standard star fields were reduced using the same algorithm. The instrumental magnitudes and colours for 116 standard star observations were compared with those given by Landolt (1992) to yield zero-points, colour terms and extinction coefficients. We found that an additional, magnitude independent, uncertainty of 0.02 mag was required to give a χ^2 of 116 for the *V*-band calibration. No such adjustment was required for $V - I$.

Each image was bias subtracted and flat-field corrected, using files constructed from twilight sky flat-field images and bias frames taken at the beginning of the same evening as the observations. The *I*-band images were combined (after determining their offsets) before using the deep coadded image for object detection. Optimal photometry was then carried out on the list of stars produced by the detection software to produce an optical catalogue for each FoV. Although the *I*-band images were combined for object detection, photometry was carried out on the individual frames. This ensures that good signal-to-noise ratio in one frame is not swamped by poor signal-to-noise ratio in another when the images are combined. The

Table 1. A sample of the photometric catalogue. The full catalogue is available from: http://www.blackwellpublishing.com/products/journals/ suppmat/MNR/MNR7160/MNR7160sm.htm, and also from the CDS. Quality flags: first character is the quality flag for the star in the *V* band, the second is for the *I* band. The meanings of the flags are: (O) OK, (N) non-stellar, (E) star too close to CCD edge, (B) background fit failed, (S) saturated, (I) ill-determined sky, (V) Variable, (F) bad (flagged) pixel, (M) negative (minus) counts.

Field No.	Index No.	α(J2000)	δ(J2000)	X	Y	V	σ_V	Quality	$V - I$	σ_{V-I}	Quality
9	3061	06 52 59.493	−24 08 58.44	1940.396	1271.814	21.660	0.933	MO	0.987	0.986	MO
2	2224	06 52 59.504	−23 52 0.84	1886.245	434.454	21.023	0.511	OO	0.574	0.539	OO
2	1028	06 52 59.506	−23 53 15.15	1885.973	619.683	18.706	0.088	OO	0.790	0.095	OO
2	1201	06 52 59.506	−23 55 37.23	1885.625	973.810	19.854	0.040	OO	1.044	0.059	OO
9	988	06 52 59.515	−24 05 17.67	1940.311	721.652	19.131	0.018	OO	0.857	0.034	OO
9	1600	06 52 59.534	−24 00 56.51	1940.473	70.826	24.385	2.898	OO	4.619	2.892	OO
9	930	06 52 59.541	−24 04 12.70	1939.621	559.756	21.411	3.731	NN	0.670	3.882	NN
9	2814	06 52 59.545	−24 07 26.56	1938.916	1042.858	24.520	1.007	OV	4.934	1.007	OV
2	4088	06 52 59.548	−24 02 37.41	1883.104	2021.075	21.370	0.706	NN	1.462	0.911	NN

individual measurements of each star are combined later, weighting each measurement according to its signal-to-noise ratio.

An astrometric solution was obtained through comparison of the optical catalogues with SuperCosmos catalogues (Hambly et al. 2001a) of the same FoVs. The root-mean squared (RMS) residuals of the 6-coefficient fit were approximately 0.2 arcsec. The resulting catalogues were then combined to produce an optical catalogue for the entire region covered by our survey, listing a position, a *V* magnitude, a *V* − *I* colour and a data quality flag (see Naylor et al. 2002) for 26 104 stars. The overlap regions between the fields were used to assess the internal consistency of the optimal photometry, which was found to be consistent at the 0.005-mag level. The final catalogue is given as Table 1. Only a sample is provided in the text; the full table is available in the online version of the journal on *Synergy*, and also via the CDS online data base. The reduction carried out here differs from that described by Naylor et al. (2002) in that an additional data quality flag has been introduced, and the flags are now indicated by character values rather than integers, since this gives greater flexibility for the format. There is also an entirely new flag, 'I', which indicates that the star's photometry is unreliable owing to ill-determined sky. The threshold for this flag to be invoked is when the fit to the sky histogram for the star has a reduced $\chi^2 > 3$. The resulting CMD is shown below in Fig. 2. A population of PMS stars is clearly visible on the CMD of the optical catalogue, lying redward of the background contamination.

3 X-RAY DATA

3.1 *ROSAT* data

Nine pointings of the *ROSAT* PSPC were made towards WR 6 between 1991 and 1992, totalling 28 ks. The data set for each pointing was retrieved from the public archives via the LEDAS website (http://ledas-www.star.le.ac.uk/rosat/) hosted by Leicester University. The data were reduced using *Asterix* version 2.3-b1, a suite of X-ray data reduction programs available from the University of Birmingham (http://www.sr.bham.ac.uk/asterix). The data were sorted into 20-arcmin radius image cylinders (spectral data was retained at this stage), excluding events recorded during periods of high background or poor aspect quality and selecting corrected pulse height (PHA) channels 11 to 201. The resulting images were then visually inspected and obvious sources masked in duplicate images, which were then used to create a background image cylinder for each pointing. These were then used, along with other calibration files supplied with the data, to create a background model for each pointing. These, and the unmasked image cylinders were then projected

to create 2D images and background models, which were used for source detection using Cash-statistic maximization in the PSS algorithm (Saxton, Ashley & Vallance 2000). The resulting source lists were then used to further mask sources in the background image cylinders to produce refined background models. The refined background models and the images were then coadded. This resulted in an image for source detection with an effective exposure time of 25.8 ks. This image was then searched for sources using PSS returning 39 X-ray sources. The archival release of *XMM–Newton* observations of this region of sky means that much of the data in this source list has been superseded in sensitivity and positional accuracy. As a result we retrieved the *XMM–Newton* data and removed from the *ROSAT* PSPC source list those objects that appeared in both sets of data.

3.2 *XMM–Newton* data

Data from two *XMM–Newton* observations using the European Photon Imaging Camera (EPIC) were used to make the X-ray source catalogue. One directed at WR 6 with 12 864 s total integration time during revolution 346 (Skinner et al. 2002), and another of 52 496 s directed at the north-west quadrant of the ring nebula S308 carried out during revolution 343 (unpublished). Skinner et al. (2002) investigated the possible existence of a close companion to WR 6. They make note of one other source in their FoV, 57.4 arcmin south of WR 6, which they fail to correlate with a SIMBAD counterpart. This source correlates with a star in our photometric PMS selection (field 1, star 73, see Table 5 later). Other than this they do not discuss the other sources in the FoV. The final EPIC source lists were retrieved from the ESA *XMM–Newton* Science Data Archive (http://xmm.vilspa.esa.es/) and filtered to remove sources with detection likelihood values of less than 20. This was to allow for an error in the calculation of detection likelihoods by the XMM–SAS pipeline, in versions 5.4.1 and earlier (see *XMM–Newton* news no. 29). The two source lists were then cross-correlated with one another to remove duplicates. In each case of a duplicate source the observation with best signal-to-noise ratio was used. The source list was then further restricted to cover just the region covered by the optical survey. The resulting source list contained 138 sources, and is given as Table 2. This table is available in full in the online version of the journal in *Synergy*, and also via the CDS online data base. Listed for each source are the *XMM–Newton* source number, right ascension, declination, error in position, count rate and error in count rate. For those X-ray sources that correlate with an optical counterpart (see Section 4) the field number and star index are also listed.
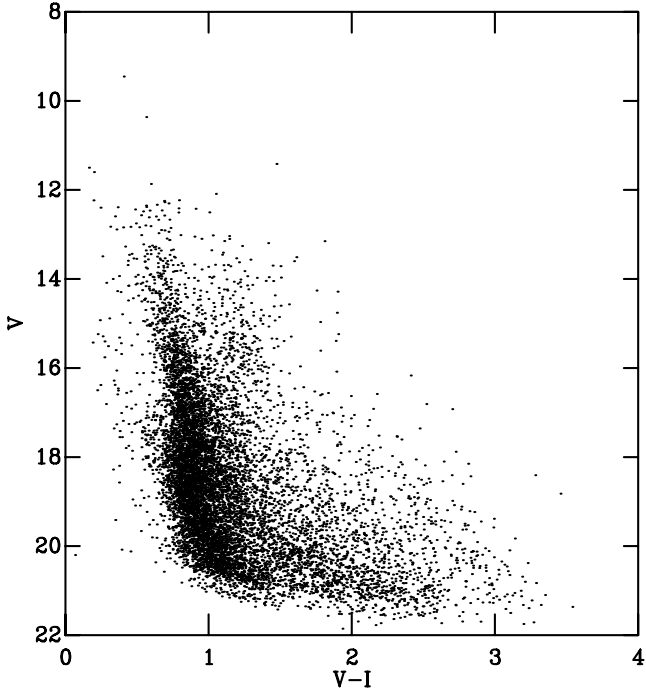
Figure 2. The CMD for the optical survey region for all unflagged objects with signal-to-noise ratio >10 in V and $V - I$.
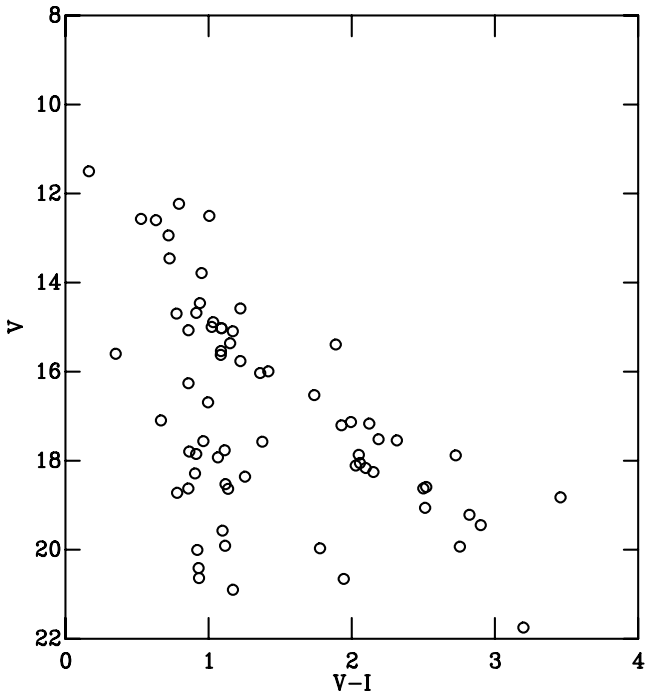
Figure 3. The CMD for X-ray correlated stars. Of the 103 stars correlated, 35 have been excluded from this plot owing to low signal-to-noise ratio (13) or for poor quality photometry (22).

Of the 39 *ROSAT* PSPC sources, 13 lay within the optical survey region and did not appear in the *XMM–Newton* source list. We will refer to this set of sources as the reduced *ROSAT* PSPC source list. This source list is given as Table 3, and is available via the CDS data base. For each source we list index number, right ascension, declination and flux. Again, for those sources that correlate with an optical counterpart we also list the field number and star index.

4 IDENTIFICATION OF X-RAY SOURCES

4.1 Cross-correlation of optical and X-ray source ists

XMM–Newton source list and the reduced *ROSAT* PSPC source list were cross-correlated against the optical catalogue. *XMM–Newton* sources were matched using a search radius of 5 arcsec, except in cases where the error in the position given in the EPIC source list was greater than this. In these cases the radius of the position error circle given in the *XMM–Newton* data was used. Since the accuracy of their positions was poorer, a search radius of 10 arcsec was used to match the *ROSAT* sources. A boresight correction of +3 arcsec in declination was applied to the *ROSAT* coordinates. This was based on the offset between the coordinates of the brightest X-ray source in the original *ROSAT* PSPC source list and the coordinates of WR 6 in the optical catalogue. Of the 151 X-ray sources in optical survey region (138 *XMM–Newton* sources and 13 *ROSAT* PSPC sources), 103 correlate with stars in the optical catalogue (91 *XMM–Newton* sources and 12 *ROSAT* PSPC sources). The positions in colour–magnitude space of the stars in the optical catalogue with X-ray correlations are shown in Fig. 3. We have excluded stars with data quality flags other than 'OO', and those with signal-to-noise ratio less than 10. It is clear from this plot that the majority of the correlated stars lie the region of the diagram occupied by the PMS. In fact, of the 68 sources plotted in Fig. 3, 43 lie in the PMS region of the diagram. The inferred X-ray fluxes for these objects are consistent with their status as PMS stars (Feigelson et al. 1993).

We estimated how many chance correlations we would expect to find in different regions of the CMD by performing the cross-correlation procedure for 8 different offsets of 30 arcsec in each axis between the catalogues. We find that we would expect up to 5 of the correlations in the PMS region of the CMD to spurious, whilst essentially all of the correlations in the background region would be spurious.

4.2 Investigation of the proper motions of the X-ray selected PMS candidates

To remove objects that were not members of the group of interest, we refined our selection to remove objects that do not share common motion. We obtained SuperCosmos proper motions for 52 stars in our X-ray selected PMS (we did not exclude stars with poor photometry flags or low signal-to-noise ratio for this experiment). A mean proper motion was calculated from the data, with each star being given a weight inversely proportional to the square of its error. Stars which contributed a $\chi^2 > 4$ were removed from the selection and the weighted mean recalculated. This was repeated until no stars in the sample contributed a χ^2 above this value. In total 17 stars were removed from the sample, and these are marked on Figs 5 and 6 with faint circles. A value of $\chi^2 > 4$ was chosen as the deselection criterion since, for a sample of 52 stars, a 2σ clip would be expected to remove 2 or 3 bonafide members of the group. It is thought that all of the stars removed from the sample were non-members. The distribution of the proper motions for the final selection are shown in Fig. 4. The width of the distribution is consistent with the mean errors and an internal velocity dispersion which is close to zero. Those objects that were classified as PMS members of an association along this sightline by both photometric and proper motion criteria are listed in Table 4. Those that were deselected based on their proper motions are listed in Table 5.

An interesting experiment would be to compare the proper motions of the confirmed members of this group of PMS stars with

Table 2. A sample of the *XMM–Newton* source list. The full list is available from: http://www.blackwellpublishing.com/products/journals/suppmat/MNR/MNR7160/MNR7160sm.htm, and also from the CDS.

Index No.	α(J2000)	δ(J2000)	σ_{pos} (arcsec)	Epic count rate$\tilde{}$(s^{-1})	σ_{CR}	Optical counterpart field no.	Star no.
1	06 54 13.040	−23 55 41.64	5.000	0.616	0.008	1	16
2	06 54 24.750	−23 50 31.56	5.000	0.034	0.005	1	10
4	06 54 28.460	−24 00 27.36	5.000	0.019	0.004	1	283
5	06 54 42.730	−24 07 14.18	5.000	0.048	0.015	8	20
6	06 54 17.530	−24 09 1.63	5.000	0.025	0.012	5	75
7	06 54 11.710	−23 56 39.57	5.000	0.011	0.005	1	73
8	06 53 48.930	−24 04 18.21	5.000	0.012	0.019	9	2086
9	06 53 13.220	−24 04 39.28	5.000	0.013	0.021	*	****
10	06 54 55.290	−23 53 38.18	5.000	0.013	0.019	3	62

Table 3. The reduced *ROSAT* source list. *X* and *Y* are positions in the PSPC FoV.

Index No.	α(J2000)	δ(J2000)	X	Y	Flux	Optical counterpart field no.	Star no.
1	06 53 1.200	−23 51 21.00	−0.270	0.070	73.169	2	2096
2	06 53 12.800	−23 53 53.00	−0.230	0.030	35.155	2	1070
3	06 53 13.200	−23 52 31.00	−0.220	0.050	36.431	2	143
5	06 53 19.600	−24 06 1.00	−0.200	−0.170	35.931	9	1029
8	06 53 28.800	−24 09 15.00	−0.160	−0.220	54.406	9	84
11	06 53 46.100	−24 07 17.00	−0.100	−0.190	39.062	9	23
15	06 53 52.900	−24 06 40.00	−0.070	−0.180	38.606	9	20
17	06 54 1.800	−24 11 42.00	−0.040	−0.270	48.397	5	3692
29	06 54 26.000	−23 43 49.00	0.050	0.200	28.123	4	216
33	06 54 38.300	−24 02 43.00	0.100	−0.120	19.837	8	343
35	06 54 43.200	−24 10 58.00	0.120	−0.250	34.905	8	26
36	06 54 49.100	−24 01 54.00	0.140	−0.100	23.722	8	116
39	06 55 12.400	−23 51 32.00	0.230	0.070	33.225	*	****

those measured by other surveys for stars along this sightline. Unfortunately the systematic error in the SuperCosmos proper motions is large at galactic latitudes $|b| \leqslant 30°$ (Hambly et al. 2001b). As such, SuperCosmos proper motions for stars within our survey region with $b \approx -10°$ will have a large systematic error. This is both magnitude and survey plate dependant.

We have assessed this issue by calculating the weighted mean of the SuperCosmos proper motions for a broad selection of background field stars in our survey. The proper motion we find is $(\mu_{\alpha \cos\delta}, \mu_{\delta}) = (2.43 \pm 0.26, -2.07 \pm 0.27)$ mas yr^{-1}. We calculate that the proper motion that would be expected due to galactic rotation and solar reflex for stars at 1 kpc distance in the direction of our survey should be approximately $(\mu_{\alpha \cos\delta}, \mu_{\delta}) = (-2, 1)$ mas yr^{-1}. Since, for a random selection of field stars, one would expect the mean proper motion to coincide with the proper motion of the LSR and solar reflex, it is clear that whilst the SuperCosmos proper motions are sufficiently internally consistent for crude membership selection, they are not suitable for drawing comparisons with proper motions obtained from other surveys.

5 DISCUSSION: HOW FAR AWAY AND HOW OLD ARE THE PMS STARS?

The fitting of theoretical isochrones to the observed PMS can yield distances and ages for stars found there. However there is a degeneracy between distance and age for low-mass stars. As such any estimates of distance and age must be made within the context of the estimates of the distances to the higher mass stars, as well as the con-

straints that higher mass stars place on the age of any associations that may be present.

Isochrones in $V/V - I$ were generated from the solar metallicity models of D'Antona & Mazzitelli (1997) in the same manner as described by Jeffries, Thurston & Hambly (2001). Empirical colour–T_{eff} conversions were obtained by fitting a 120-Myr isochrone to the Pleiades at a distance modulus of 5.6, $E(B - V) = 0.04$, $E(V - I_c) = 0.05$.

We scaled the resultant isochrones for a distance of 600 pc, in keeping with the distance derived for Cr 121 by de Zeeuw et al. (1999) of 592 ± 28 pc. In addition to shifting the isochrones for distance, they were also shifted for an extinction of $A_V = 0.17$ (Kaltcheva 2000). This corresponds to a reddening of $E(V - I) = 0.07$ (if we assume a galactic reddening law), though this has little effect on the results as the reddening vector lies along the isochrones. If the low-mass PMS stars are located within the association at the distance found from the *Hipparcos* data, the best fitting isochrones are those corresponding to ages between 20 and 50 Myr (see Fig. 5). These imply a median age of 30 Myr, with an age spread of about 30 Myr. Such an age spread is not considered likely for an association of this age (Jeffries & Tolley 1998, and references therein). Additionally, as was noted by de Zeeuw et al. (1999), the presence of an O star and early B stars indicates that this moving group is young, about 5 Myr in age. For such a large number of PMS stars to be found within such a small survey region would also be surprising if they were associated with the group described by de Zeeuw et al. (1999). Assuming a Salpeter initial mass function (IMF), we calculate that we would expect to find 3900 0.20–0.73 M$_\odot$ ($14 \leqslant V \leqslant 20$
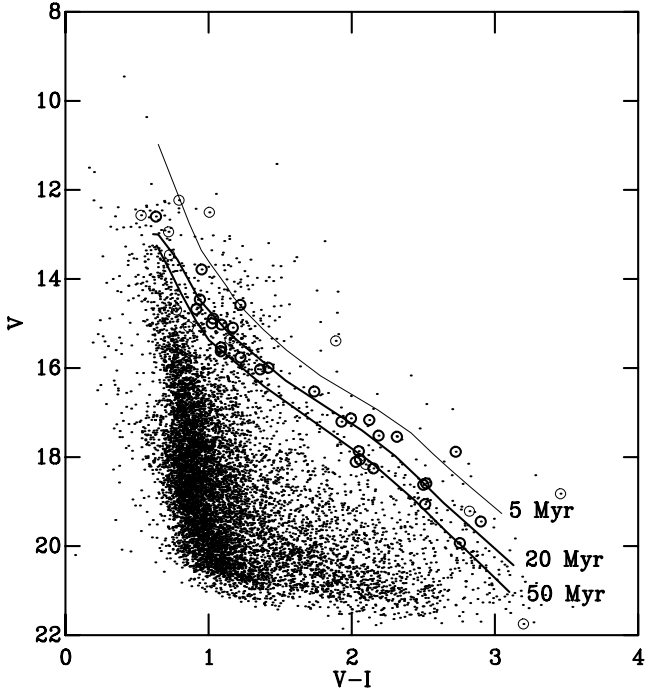
Figure 4. The proper motions for our X-ray-selected PMS. Black dots show SuperCosmos proper motions for individual stars (Hambly et al. 2001), whilst the black error diamond indicates their weighted mean. The mean error in the SuperCosmos proper motions is 9.7 mas yr^{-1} in $\mu_{\alpha\cos\delta}$ and 8.3 mas yr^{-1} in μ_δ.

at 592 pc) stars for the 85 B stars selected as members by de Zeeuw et al. (1999). If we assume that these would be distributed evenly over a region at least as large as the $13° \times 16°$ region occupied by the B stars, then we would expect to find fewer than five 0.20–0.73 M$_\odot$ stars within the region observed here. As such, the PMS found here would represent quite a concentration of the low-mass stars of the association. It should be noted that a more realistic IMF would predict even fewer stars in this mass range, since several observational studies have found that the IMF in young clusters flattens out at masses below ∼0.8 M$_\odot$ (e.g. Preibisch et al. 2002; Briceño et al. 2002, and references therein).

The three lines of argument described above lead us to reject the scenario in which the low-mass PMS stars are associated with the moving group detected using the *Hipparcos* data. Instead, we use the presence of early-type main sequence B-stars in the membership lists for both interpretations of Cr 121 to constrain the age to less than 15 Myr. Such a low age is also more in keeping the scatter of stars in the PMS region of the diagram. Scaling sets of isochrones for ages of less than 15 Myr for distance until they fitted as much of the data as possible gave a distance of 1050 pc, and a modal age of between 1 and 10 Myr, applying the same extinction as before. This is consistent with the distance given by Kaltcheva (2000) for a compact group of stars at 1085 ± 41 pc. Fig. 6 shows that the age spread implied by fitting isochrones for this distance is less than 10 Myr, much more in keeping with age spreads observed in other young clusters and associations (e.g. Pozzo et al. 2003) than the 30 Myr age spread suggested by the fit for 600 pc. Isochrones for 1 and 20 Myr, scaled for the same distance as the 5 and 10 Myr ones, are included in Fig. 6 for comparison.

If we carry out a similar calculation to the one above, using a Salpeter IMF, we find that we would expect there to be around 540 stars in the 0.29–0.98 M$_\odot$ mass range ($14 \leqslant V \leqslant 20$ at 1050 pc)
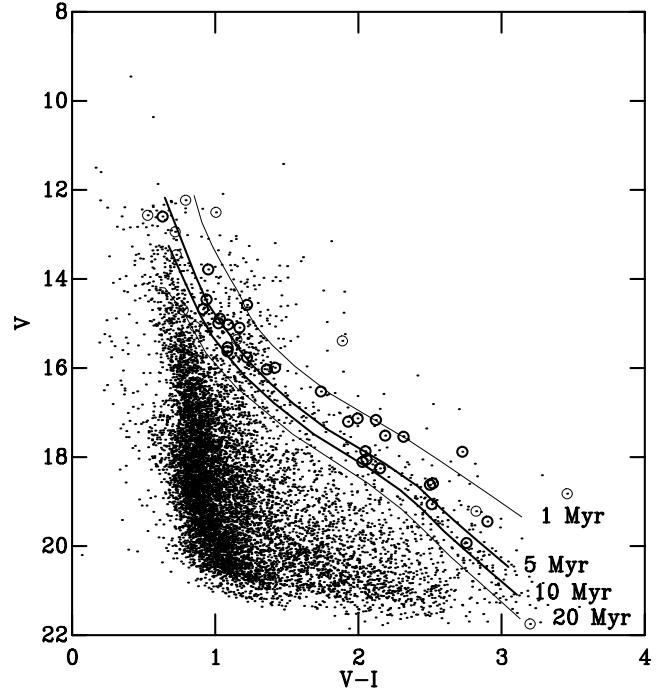
Figure 5. The CMD for the fields centred on WR 6 with 5, 20 and 50 Myr isochrones overlaid for (intrinsic) d$M = 8.9$ and $A_V = 0.17$. Circled points indicate X-ray correlated stars. Points marked with faint circles are those cut from the sample in Section 4.2.
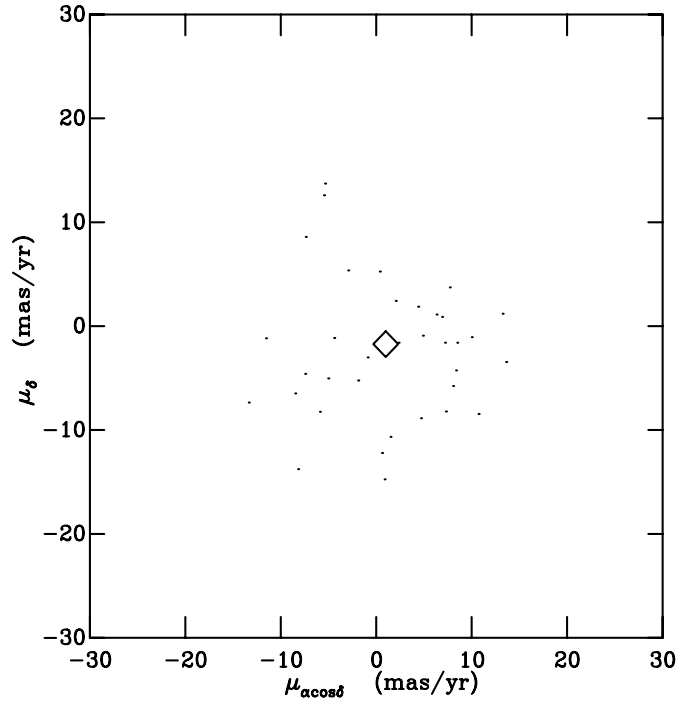
Figure 6. The CMD for the fields centred on WR 6 with 1, 5, 10 and 20 Myr isochrones fitted for (intrinsic) d$M = 10.1$ and $A_V = 0.17$. Circled points indicate X-ray-correlated stars. Points marked with faint circles are those cut from the sample in Section 4.2.

for the 11 B-type members of the more distant cluster suggested by Kaltcheva (2000). If we assume an even distribution of stars over the $\approx 1°$ radius surveyed there, then we would expect to find, at most, 130 stars in this mass range in the region covered by our

Table 4. The catalogue of X-ray-selected PMS stars which were also proper motion members. Quality flags: first character is the quality flag for the star in the *V* band, the second is for the *I* band. The meanings of the flags are: (O) O.K., (N) non-stellar, (E) star too close to CCD Edge, (B) Background fit failed, (S) Saturated, (I) ill-determined sky, (V) Variable, (F) bad (Flagged) pixel, (M) negative (Minus) counts.

Field No.	Index No.	α(J2000)	δ(J2000)	X	Y	V	σ_V	Quality	$V - I$	σ_{V-I}	Quality
1	283	06 54 28.382	−24 00 28.33	523.465	1702.193	17.519	0.040	OO	2.187	0.040	OO
8	20	06 54 42.700	−24 07 14.57	1690.619	1010.048	13.786	0.006	OO	0.951	0.008	OO
3	62	06 54 55.245	−23 53 38.92	1278.492	679.337	14.680	0.006	OO	0.914	0.008	OO
8	114	06 54 49.326	−24 01 45.58	1465.167	190.009	17.544	0.010	OO	2.315	0.012	OO
1	241	06 54 23.176	−23 58 27.34	701.341	1400.640	15.763	0.018	OO	1.222	0.019	OO
1	217	06 53 44.112	−23 56 33.98	2036.446	1119.018	17.868	0.038	OO	2.049	0.038	OO
1	103	06 53 53.358	−24 02 6.55	1719.630	1947.546	14.996	0.003	OO	1.022	0.005	OO
1	142	06 54 17.023	−23 51 19.34	911.908	333.942	17.132	0.009	OO	1.994	0.012	OO
5	146	06 54 30.847	−24 03 21.67	416.553	414.314	15.993	0.006	OO	1.417	0.009	OO
1	270	06 54 4.895	−24 00 1.90	1325.816	1636.559	16.527	0.024	OO	1.738	0.025	OO
5	155	06 54 24.476	−24 03 46.10	634.082	475.192	17.206	0.008	OO	1.928	0.011	OO
5	175	06 54 28.227	−24 05 50.53	506.052	785.303	15.538	0.006	OO	1.086	0.009	OO
5	377	06 54 11.396	−24 04 35.61	1080.652	598.685	18.591	0.013	OO	2.520	0.015	OO
9	65	06 53 49.227	−24 05 44.12	243.212	786.842	15.093	0.004	OO	1.169	0.006	OO
1	669	06 54 23.934	−24 00 56.84	675.375	1773.234	18.256	0.008	OO	2.151	0.010	OO
2	610	06 53 23.910	−23 58 34.80	1051.277	1415.663	18.623	0.080	OO	2.500	0.090	OO
2	128	06 53 26.487	−23 51 38.56	963.496	378.178	17.167	0.033	OO	2.122	0.033	OO
8	59	06 54 53.249	−24 06 16.99	1330.721	866.268	15.025	0.006	OO	1.090	0.008	OO
1	711	06 54 30.531	−24 02 11.12	450.042	1958.374	19.059	0.012	OO	2.512	0.014	OO
1	421	06 54 20.499	−23 52 31.25	792.979	513.154	19.931	0.031	OO	2.755	0.033	OO
2	28	06 53 45.803	−24 00 4.24	303.310	1638.443	13.306	0.012	FO	0.711	0.016	FO
2	310	06 53 39.902	−23 49 58.21	504.650	127.940	19.901	0.249	IO	2.729	0.264	IO
6	26	06 55 5.986	−23 48 6.44	886.951	1570.648	12.598	0.008	OO	0.632	0.009	OO
1	243	06 54 32.055	−23 58 39.95	397.960	1432.076	15.624	0.017	OO	1.085	0.018	OO
2	123	06 53 14.140	−23 51 12.99	1385.775	314.702	18.053	0.054	OO	2.057	0.055	OO
1	50	06 54 4.958	−23 51 58.68	1324.456	432.186	14.461	0.013	OO	0.939	0.014	OO
2	126	06 52 59.607	−23 51 31.79	1882.788	362.056	17.881	0.048	OO	2.726	0.048	OO
1	62	06 53 58.401	−23 53 50.12	1548.458	710.112	14.581	0.013	OO	1.222	0.015	OO
4	367	06 54 1.454	−23 38 28.39	1416.782	120.055	18.109	0.018	OO	2.028	0.020	OO
4	18	06 53 59.247	−23 42 24.56	1491.916	708.767	10.623	0.011	IN	0.015	0.015	IN
4	343	06 54 26.122	−23 37 49.12	571.728	21.888	19.264	0.142	OO	2.538	0.142	OO
4	380	06 54 14.114	−23 38 48.92	983.074	171.002	19.447	0.023	OO	2.901	0.025	OO
9	84	06 53 28.076	−24 09 18.79	965.046	1321.824	14.888	0.006	OO	1.032	0.008	OO
8	26	06 54 43.492	−24 11 0.44	1663.026	1572.877	11.588	0.011	NN	0.138	0.016	NN
8	116	06 54 49.690	−24 01 54.07	1452.693	211.155	16.031	0.007	OO	1.360	0.008	OO

optical survey. This is consistent with the population of the PMS observed here. This would indicate that the PMS we have identified consists of stars in the ≈1 kpc distant cluster identified by Collinder (1931), Eggen (1981) and Kaltcheva (2000). To avoid confusion we shall refer to this distant cluster as Cr 121, and we shall refer to the association at approximately 600 pc as CMa OB2, following Eggen (1981).

6 CONCLUSIONS

It seems clear that the low-mass PMS stars detected here are associated with the compact group of stars found by Kaltcheva (2000), Eggen (1981) and Collinder (1931) at a distance of over 1 kpc, originally designated Cr 121. If this cluster were of the extent and at the distance found by de Zeeuw et al. (1999), the discovery of such a concentration of low-mass PMS stars which are so much older than the rest of the association, and with an age spread of 30 Myr, seems incredible. It is also clear however, that there is a young moving group that was detected using the *Hipparcos* data by de Zeeuw et al. (1999) at a distance of 592 ± 28 pc, of which WR 6 is likely a member, in the same direction. The characteristics of the group described there, however, seem more in keeping with an OB association, than with the compact open cluster originally described as Cr

121. We argue that the distant open cluster should retain its original designation as Collinder 121, whilst the nearer OB association described by Feinstein (1967), de Zeeuw et al. (1999) and Dias et al. (2002) should be re-designated as CMa OB2, following Eggen (1981).

Whilst the *Hipparcos* census of OB associations within 1 kpc is an invaluable resource for studying recent local star formation, this work demonstrates the importance of interpreting proper-motion and parallax data within the context of age and distance constraints imposed by main-sequence high-mass and low-mass PMS stars. This is particularly true when investigating structures that extend beyond the range of the *Hipparcos* data.

Table 5. The catalogue of X-ray-selected PMS stars that were not proper motion members. Quality flags: first character is the quality flag for the star in the *V* band, the second is for the I band. The meanings of the flags are: (O) O.K, (N) non-stellar, (E) star too close to CCD Edge, (B) Background fit failed, (S) saturated, (I) ill-determined sky, (V) variable, (F) bad (Flagged) pixel, (M) negative (Minus) counts.

Field No.	Index No.	α(J2000)	δ(J2000)	X	Y	V	σ_V	Quality	$V - I$	σ_{V-I}	Quality
1	10	06 54 24.926	−23 50 32.22	641.610	216.465	12.291	0.011	NN	0.974	0.016	NN
5	75	06 54 17.359	−24 09 2.91	876.917	1264.800	13.457	0.006	OO	0.727	0.008	OO
1	73	06 54 11.668	−23 56 39.46	1094.679	1131.870	15.363	0.006	OO	1.150	0.009	OO
1	54	06 54 38.612	−23 52 46.11	173.600	550.238	14.697	0.005	OO	0.776	0.006	OO
4	32	06 54 25.237	−23 48 13.95	602.029	1579.247	10.399	0.011	II	0.530	0.015	II
9	10	06 53 47.900	−24 04 14.41	288.466	563.284	12.941	0.008	OO	0.720	0.011	OO
1	527	06 54 34.361	−23 56 31.49	319.100	1111.931	19.216	0.019	OO	2.822	0.021	OO
5	474	06 54 15.829	−24 07 41.69	929.199	1062.385	19.367	0.145	OO	2.456	0.158	OO
1	198	06 54 2.020	−23 55 24.62	1424.525	945.530	18.823	0.014	OO	3.458	0.016	OO
8	825	06 54 35.539	−24 01 26.02	1936.076	141.717	21.748	0.087	OO	3.199	0.089	OO
8	45	06 55 1.219	−24 03 24.50	1058.879	436.294	15.070	0.006	OO	0.859	0.009	OO
4	25	06 53 47.103	−23 44 23.71	1907.386	1006.131	12.502	0.011	OO	1.005	0.016	OO
2	51	06 53 1.832	−23 51 36.62	1806.706	373.990	15.391	0.016	OO	1.888	0.017	OO
4	28	06 54 1.644	−23 46 13.73	1409.453	1279.888	11.039	0.011	II	1.214	0.015	II
4	29	06 53 48.959	−23 46 15.28	1843.567	1284.157	12.570	0.011	OO	0.528	0.013	OO
9	23	06 53 46.731	−24 07 19.32	328.471	1024.081	12.231	0.005	OO	0.793	0.007	OO
5	3692	06 54 2.434	−24 11 47.66	1385.935	1675.635	20.010	0.275	NI	4.027	0.278	NI
4	216	06 54 26.372	−23 43 44.89	563.172	908.619	18.164	0.011	OO	2.097	0.014	OO

REFERENCES

Briceño C., Luhman K. L., Hartmann L., Stauffer J. R., Kirkpatrick J. D., 2002, ApJ, 580, 317

Collinder P., 1931, Annals Obs. Lund, 2, 1

D'Antona F., Mazzitelli I., 1997, Mem. Soc. Astron. Ital., 68, 807

de Zeeuw P. T., Hoogerwerf R., de Bruijne J. H. J., Brown A. G. A., Blaauw A., 1999, AJ, 117, 354

Dias W. S., Lépine J. R. D., Alessi B. S., 2001, A&A, 376, 441

Dias W. S., Alessi B. S., Moitinho A., Lépine J. R. D., 2002, A&A, 389, 871

Dolan C. J., Mathieu R. D., 2001, AJ, 121, 2124

Eggen O. J., 1981, ApJ, 247, 507

Feigelson E. D., Casanova S., Montmerle T., Guibert J., 1993, ApJ, 416, 623

Feinstein A., 1967, ApJ, 149, 107

Hambly N. C., Davenhall A. C., Irwin M. J., MacGillivray H. T., 2001, MNRAS, 326, 1315

Hambly N. C. et al., 2001, MNRAS, 326, 1279

Jeffries R. D., Tolley A. J., 1998, MNRAS, 300, 331

Jeffries R. D., Thurston M. R., Hambly N. C., 2001, A&A, 375, 863

Kaltcheva N. T., 2000, MNRAS, 318, 1023

Landolt A. U., 1992, AJ, 104, 340

Melnik A. M., Efremov Y. N., 1997, VizieR Online Data Catalog, 902, 10013

Naylor T., 1998, MNRAS, 296, 339

Naylor T., Fabian A. C., 1999, MNRAS, 302, 714

Naylor T., Totten E. J., Jeffries R. D., Pozzo M., Devey C. R., Thompson S. A., 2002, MNRAS, 335, 291

Pozzo M., Jeffries R. D., Naylor T., Totten E. J., Harmer S., Kenyon M., 2000, MNRAS, 313, L23

Pozzo M., Naylor T., Jeffries R. D., Drew J. E., 2003, MNRAS, 341, 805

Preibisch T., Brown A. G. A., Bridges T., Guenther E., Zinnecker H., 2002, AJ, 124, 404

Saxton R. D., Ashley J., Vallance R., 2000, ASTERIX Data Analysis, User Note 005. School of Physics and Astronomy, Birmingham University

Skinner S. L., Zhekov S. A., Güdel M., Schmutz W., 2002, ApJ, 579, 764

This paper has been typeset from a TEX/LATEX file prepared by the author.